JBC Papers in Press. Published on November 9, 2010 as Manuscript M110.126425
The latest version is at http://www.jbc.org/cgi/doi/10.1074/jbc.M110.126425

THE RUN DOMAIN OF RUBICON IS IMPORTANT FOR HVPS34 BINDING, LIPID KINASE INHIBITION AND AUTOPHAGY SUPRRESSION

Qiming Sun[1], Jing Zhang[1], Weiliang Fan[1], Kwun Ngok Wong[1], Xiaojun Ding[2], She Chen[2], and Qing Zhong[1]

From Division of Biochemistry and Molecular Biology[1], Department of Molecular and Cell Biology, University of California at Berkeley, Berkeley, CA 94720, USA. National Institute of Biological Sciences[2], Beijing, 102206, China

Running head: Role of the Rubicon RUN domain in Autophagy

Address correspondence to: Qing Zhong, Ph.D., Department of Molecular and Cell Biology, The University of California at Berkeley. 316 Barker Hall, Berkeley, CA 94720. Tel: 510-6436842. Fax: 510-6427038. E-mail: qingzhong@berkeley.edu

The Class III phosphatidylinositol 3-kinase (PI3KC3) plays a central role in autophagy. Rubicon, a RUN-domain containing protein, is newly identified as a PI3KC3 subunit through its association with Beclin 1. Rubicon serves as a negative regulator of PI3KC3 and autophagosome maturation. The molecular mechanism underlying the PI3KC3 and autophagy inhibition by Rubicon is largely unknown. Here, we demonstrate that Rubicon interacts with the PI3KC3 catalytic subunit hVps34 via its RUN domain. The RUN domain contributes to the efficient inhibition of Rubicon on PI3KC3 lipid kinase activity. Further, a Rubicon RUN domain deletion mutant fails to complement the autophagy deficiency in Rubicon depleted cells. Hence, these results reveal a critical role of the RUN domain for Rubicon in PI3KC3 and autophagy regulation.

PI3KC3 is essential for autophagy, protein sorting, phagosome maturation and cytokinesis (1-4). The class III PI3K is composed of the catalytic subunit hVps34 and two regulatory subunits p150 and Beclin 1 that are highly conserved from yeast to human. Functional equivalents of Beclin 1/hVps34/p150 in yeast -Atg6/Vps15/Vps34 are essential for autophagy and vacuolar protein sorting (3,5). The specificity of PI3KC3 in yeast is determined by different complex compositions. Two regulatory proteins, Atg14 and Vps38, direct the core PI3K complex to either the pre-autophagosome structure for autophagy or the endosome for vacuolar protein sorting (3,6), respectively.

Along with several other groups, we have recently purified a mammalian PI3KC3 holocomplex that includes hVps34, p150, Beclin 1, UVRAG, Barkor/Atg14(L), and Rubicon (also called p120 or Baron) (7-12). PI3KC3 forms two mutually exclusive protein subcomplexes that localize to different subcellular organelles and execute distinct functions. One complex is composed of the PI3KC3 core complex (hVps34, p150, and Beclin 1) and Barkor/Atg14(L). Barkor/Atg14(L), and is the targeting factor for this complex to nascent autophagosomes (7). The other complex consists of the PI3KC3 core complex and UVRAG. UVRAG positively regulates PI3KC3 activity and autophagy maturation (13). UVRAG is also required for endocytosis through its interaction with C-VPS/HOPS (13,14). Rubicon (*Ru*n domain protein as *B*eclin 1 *i*nteracting and *c*ysteine-rich c*on*taining) is a newly identified PI3KC3 subunit (7-12). It serves as a negative regulator of autophagosome and endosome maturation (9,10,12).

Understanding the functional mode and structure basis of Rubicon in autophagy is crucial. Here we demonstrate that Rubicon resides in the UVRAG subcomplex of PI3KC3. Interestingly, we detected no direct interaction between Rubicon and Beclin 1 although it was originally purified in the Beclin 1 complex. Instead, Rubicon physically interacted with UVRAG and hVps34. We have mapped the interaction domain of Rubicon with hVps34 to the RUN domain. The RUN domain is critical for Rubicon's function in suppressing PI3KC3 lipid kinase activity and autophagy maturation.

EXPERIMENTAL PROCEDURES

Cell Culture-293T and U_2OS cells were cultured in DMEM supplemented with 10% FBS. For the tetracycline-inducible cells, Tet-approved FBS (Clontech) was used. For immunoprecipitation, cell extracts were incubated with 2 μg of antibody for 4 h and collected with protein A–Sepharose beads (Amersham Biosciences) for 4 h at 4 °C. The immunocomplexes were then washed three times and subjected to SDS-PAGE. Immunoblotting was performed following standard procedures.

Plasmids and antibodies-The full-length cDNA for human Rubicon (KIAA0226) was generated by PCR on the basis of a partial cDNA clone purchased from Kazusa. Rubicon antibodies were generated by Abmart, Abgent and Cell Signaling Inc. Other antibodies used in this study include anti-FLAG (M2; Sigma), anti-HA (Roche), anti-Myc (9E10; Santa Cruz Biotechnology), anti-Tubulin (Santa Cruz Biotechnology), anti-UVRAG (Abgent), and anti-LC3 (Sigma). pCDNA5/FRT/TO (Invitrogen) was modified by introducing the coding sequence of 3xFLAG tag (between NotI and XhoI) and designated as pCDNA5-FLAG. The Rubicon coding sequence was inserted between BamHI and NotI to generate the reading frame of Rubicon-FLAG, which was used for setting up a stable cell line. pCDNA4/TO (Invitrogen) was modified by introducing the coding sequence of Myc tag (between NotI and XhoI) and designated as pCDNA4-Myc, into which Rubicon coding sequence were cloned between BamHI and NotI. The information about other recombinant constructs applied in this study was summarized in supplementary table 1.

PI3K kinase assay-The procedure was modified from a protocol described before (13). FLAG-tagged hVps34 expressed in cells was immunoprecipitated with M2 beads (Sigma) and extensively washed and pre-incubated at room temperature for 10 min in a 60μl of reaction containing 2μg of sonicated phosphatidylinositol. The reaction was initiated with addition of 5μl of ATP mixture (1μl 10mM unlabeled ATP, 1μl γ-^{32}P-ATP and 3μl H_2O) and incubated for 15 min at room temperature. The reaction was terminated and dried with SpeedVac and resuspended in 20 μl $CHCl_3$:MeOH (1:1). The resultant assay product was separated on dried silica aluminum thin liquid chromatography plates with running buffer ($CHCl_3$: MeOH: 4M NH_4OH; 9:7:2). Radiolabeled PtdIns-3-P was visualized with a Fuji Phosphor Imager scanner.

Recombinant protein purification-The protocol for recombinant protein production from insect cells is similar to a TAP procedure described before (7). For the recombinant proteins purified from mammalian cells, whole-cell lysates from transfected 293T cells were prepared in TAP buffer, recombinant proteins were collected by M2 beads. After extensive washing, the proteins were eluted by FLAG peptide (0.1mg/ml) and analyzed.

Immunostaining-Cells were grown on 6-well plates with coverslips. One day later, cells were fixed with 4% paraformaldehyde solution in PBS at room temperature for 10 min. After permeabilization with PBS buffer containing 0.1% Triton X-100 at room temperature for 20 min, cells were incubated with primary antibodies at 37 °C for 2 h. Upon extensive washing, cells were incubated with different fluorescent dye conjugated secondary antibodies at 37 °C for 2 h. Slides were examined by using a laser scanning confocal microscope (Zeiss LSM 510 META UV/Vis).

Inducible shRNA and complementation Cell Lines-The shRNA sequences were designed with ‘‘siRNA Target Finder’’ provided by Ambion and were cloned into BglII and HindIII sites of pSuperior.puro vector (Oligoengine). The inducible shRNA cell lines were established according to the protocol. The shRNA coding sequence for human Rubicon knockdown is GATCCCC GCAGTGGAACAGAACAACCTTCAAA GAGGTTGTTCTGTTCCACTGCTTTTTA. The targeted sequence of Rubicon is underlined. The inducible knockdown stable cell lines were generated from U_2OS^{TetR} cells (7). To measure the knockdown efficiency, cells were treated with 500ng/mL

Doxycycline (DOX) for 3 days followed by Western blotting against Rubicon. In complementation assays, RNAi resistant wild type and mutants of Rubicon (in pCDNA4-GFP-FLAG) were generated by site-specific mutagenesis with the primes p1: catgctgcagtgcctggaagcCgtCgaGcaAaaTaaTc cccgcctcctggctcagatc and p2: gatctgagccagg aggcggggAttAttTtgCtcGacGgcttccaggcactgc agcatg. Theses constructs were expressed in Rubicon depleted cells and stable cell lines were established by selection against 200μg/ml Zeocin, 0.5μg/ml Blasticidin and 1μg/ml puromycin.

Transmission Electron Microscope analysis-For electron microscopy, cells were fixed with 2% glutaraldehyde in 0.1M Sodium cacodylate buffer (pH 7.2) for two hours followed by 1% Osmium tetroxide in 0.1M sodium cacodylate buffer (pH 7.2) 2 hours. Samples were blocked with 0.5% aqueous Uranyl Acetate overnight and treated by low temperature dehydration and infiltration with a graded series of Epon/Araldite, which were followed by the embedment in 100% Epon/Araldite. Thin section (60nM) were cut and stained with Reynalds lead citrate and FEI Tecnai 12 Transmission electron microscope.

RESULTS

Compositions of two mutually exclusive PI3KC3 complexes. The PI3KC3 complex has recently been purified by several groups in mammalian cells (7-11). In addition to the catalytic subunit hVps34, the regulatory subunit p150, Beclin 1, UVRAG, and Barkor/Atg14(L), a novel protein called Rubicon (*Ru*n domain protein as *B*eclin 1 *i*nteracting and *c*ystein-rich c*on*taining) was also identified in this complex (7,9,10). Rubicon is involved in autophagosome maturation and likely involved in endosome maturation also (9,10). Rubicon contains 972 amino acids, with a coiled-coil domain, a FYVE-like domain, and a recognizable RUN domain that is shared by a group of proteins interacting with small GTPases (15-17),.

The stoichiometry of the PI3KC3 complex is complicated by the formation of two mutually exclusive subcomplexes characterized by Barkor/Atg14(L) and UVRAG respectively (7,8). Two subcomplexes have organelle specific distributions. The Barkor/Atg14(L) complex is localized to autophagosomes (7,8), while the UVRAG complex predominantly resides on endosomes (14). Although Rubicon is identified as a component of PI3KC3, it is still not clear which PI3KC3 subcomplex it associates with or whether it forms a unique subcomplex of PI3KC3. To clarify this question, we performed sequential affinity purifications of Rubicon cellular complexes to elucidate its complex compositions.

Rubicon (ZZ-Rubicon-FLAG) was used as bait (Fig.1A) to purify its endogenous complex following a procedure described before in U_2OS cells (7,11,18). In the Rubicon complex, UVRAG, hVps34, p150 and Beclin 1, but not Barkor/Atg14(L), were detected by mass spectrometry (Fig. 1A). Rubicon consistently coprecipitated with hVps34 (Fig. 1B). These data confirmed the presence of Rubicon in the PI3KC3 complex, and assigned Rubicon to the subcomplex with UVRAG.

Rubicon directly binds to UVRAG and hVps34. Although Rubicon has been shown to interact with the PI3KC3 complex (Fig. 1) (9,10), the component through which it directly binds to PI3KC3 has not been characterized. To test which component(s) of PI3KC3 directly interact with Rubicon, we purified recombinant full-length Rubicon, hVps34, UVRAG, Beclin 1 and Barkor/Atg14(L) from baculovirus-infected insect cells or mammalian cells (Fig. 2A), and tested their interactions in an *in vitro* pull-down assay. All of these recombinant proteins were purified to near homogeneity (Fig. 2A). Both Rubicon and Barkor/Atg14(L) possess an additional 6xHis tag. These two proteins were bound to a Ni-NTA column first, followed by incubation of individual PI3KC3 subunits. In this *in vitro* pull-down assay, Rubicon directly bound to hVps34 and UVRAG (Fig. 2B). Interestingly, there was no direct interaction between Rubicon and Beclin 1, although Rubicon was identified in the

Beclin 1 complex (9,10). As a control, we found that Barkor/Atg14(L) interacted with Beclin 1 but neither hVps34 nor UVRAG bound directly (Fig. 2B).

The RUN domain of Rubicon interacts with hVps34. We mapped the interaction domain of Rubicon for UVRAG and hVps34 binding. A series of Rubicon deletion mutants were generated, including mutants deleting the RUN domain, coiled-coil domain (CCD), or FYVE-like domain from full-length Rubicon respectively, as well as three large polypeptide fragments containing the RUN domain, CCD or FYVE domain (Fig 3A). The interaction of these mutants with UVRAG was evaluated by an immuno-precipitation assay. Deletion of the RUN domain, CCD, or FYVE-like domain was not enough to abolish the interaction between Rubicon and UVRAG (Fig. 3A, lanes 3-5). Two fragments of Rubicon encompassing amino acids aa300-600 and aa600-972, but not the N-terminal fragment aa1-300, could interact with UVRAG efficiently (Fig. 3A), which is consistent with the previous report that a large region (aa393-849) of Rubicon binds to UVRAG (9).

Since we detected a direct interaction between Rubicon and hVps34, we further investigated Rubicon's interaction domain with hVps34. The C-terminus of Rubicon (aa300-972) could pull down hVps34 probably through UVRAG (Fig. S1) (9,10). Unexpectedly, the N-terminal region of Rubicon (aa1-300) that has no interaction with UVRAG (9,10), strongly bound to hVps34 in the co-immunoprecipitation assay (Fig. 3B). We further divided the first 300 amino acids into three fragments including the RUN domain alone (aa49-180). Although the expression of the RUN domain alone is much lower than the other two fragments, the weakly expressed RUN domain bound to hVps34 strongly (Fig. 3B).

The RUN domain contributes to Rubicon inhibition on hVps34 lipid kinase activity. The binding of Rubicon RUN domain to hVps34 led to a speculation that the RUN domain might be involved in PI3KC3 regulation. We measured PI3KC3 lipid phosphorylation activity in HEK293T cells expressing wild type or mutant forms of Rubicon. PI3KC3 phosphorylates the 3′-hydroxyl position of the phosphatidyl-inositol (PtdIns) ring to produce PtdIns3P (PI3P) (19,20). The production of PI3P by PI3KC3 could be visualized and quantified by fluorescence of the GFP-tagged double FYVE finger of the Hrs protein (15). Because the FYVE probe specifically binds to PI3P, we could measure PI3KC3 activity by detecting FYVE fluorescence. PI3P production was compromised in Rubicon expressing cells compared to that in wild-type cells (Fig. 4A and 4B), consistent with its inhibitory role on PI3KC3 lipid phosphorylation (10). We then expressed different fragments of Rubicon to test their effect on PI3KC3 activity. Since the expression of the RUN domain alone was low probably because its expression requires the surrounding regions (Fig. 3B), we expressed the N-terminus of Rubicon (aa1-300) and a large C-terminus (aa180-972) to score their effect on PI3P production. The RUN domain-containing fragment was efficient in suppressing PI3P production (Fig. 4A and 4B), suggesting that the Rubicon binding of hVps34 via the RUN domain plays an important role in hVps34 inhibition. As a positive control, PI3P production could be efficiently blocked by treatment of the PI3K inhibitor 3-methyladeline (3-MA) (Fig. 4A and 4B). In addition, the N-terminus of Rubicon also reduced the number of LC3 puncta (Fig. S2), suggesting that autophagy is also blocked by this fragment.

To consolidate the function of the Rubicon RUN domain in PI3KC3 regulation, we measured the lipid phosphorylation activity in an *in vitro* TLC lipid kinase assay. In this assay, the production of PI(3)P by PI3KC3 could be detected and quantified by radiolabeling the phosphate group of phosphoinositol (19,20). hVps34 was coexpressed with Barkor/Atg14(L), UVRAG and Rubicon (Fig. 4C), and its lipid kinase activity was tested accordingly. Both Barkor/Atg14(L) and UVRAG stimulated hVps34 lipid kinase activity (Fig.

4D), supporting their positive roles in hVps34 activation. Co-expression of wild-type Rubicon efficiently blocked UVRAG-mediated hVps34 activity (Fig. 4D, lane 4), indicating that Rubicon could antagonize the UVRAG-mediated hVps34 stimulation. A Rubicon mutant with RUN domain deletion significantly reduced the inhibitory activity of Rubicon on PI3P production (about 40%) (Fig. 4D, lane 5). This suggests that the RUN domain of Rubicon contributes to its efficient suppression of PI3KC3 lipid kinase activity.

The RUN domain is important for Rubicon's function in autophagy. Two recent studies suggested that Rubicon plays a negative role in autophagosome maturation (9,10). We aimed to investigate the function of the RUN domain in autophagy regulation. We employed two of the most representative approaches for autophagy regulation, electron microscopic analysis and p62 degradation, to study the structural requirement of the RUN domain in autophagy.

In Rubicon depleted cells, autophagosome maturation is promoted, which leads to the accumulation of late autophagic vacuoles, probably due to inability of lysosomes to digest increased autophagosomes in time. Autophagic vacuoles could be detected under the Electron Microscope (EM). We performed the electron microscopic analysis in Rubicon wild type and RNAi depleted cells. Rubicon was depleted by a short hairpin RNA (shRNA) against Rubicon that was inducibly expressed upon the addition of Doxycycline (DOX) in U_2OS cells. In Rubicon depleted cells, we observed abundant mature autophagic vacuoles that are highly enriched in cytosolic contents and organelles (Fig. 5A, marked by arrows). Autophagic vacuoles were rarely observed in U_2OS parental or shRNA non-induced cells (Fig. 5A). This observation is consistent with the published results (9,10).

Rubicon depletion also led to the accumulation of LC3 cytosolic puncta representing autophagic vacuoles (Fig. S3). A significant portion of LC3 cytosolic puncta colocalized with Rab5 (early endosome marker), Rab7 (late endosome marker) and LAMP1 (lysosome marker) (Fig. S1), suggesting that late autophagic vacuoles that fuse with endosomes and lysosomes were accumulated in Rubicon depleted cells. These data confirmed that autophagosome maturation is accelerated when Rubicon is depleted, consistent with published results (9,10).

We further tested if ectopically expressed Rubicon could slow autophagosome maturation therefore relieve the accumulation of mature autophagic vacuoles. We established Rubicon RNAi depleted cells stably complemented with RNAi resistant wild type Rubicon (Fig. S4). Rubicon RUN deletion (aa1-180 deletion) or C-terminal deletion (CT, aa800-972 deletion) mutants were also stably expressed in Rubicon depleted U_2OS cells. Autophagic vacuoles were observed and counted in these cells under the EM. Expression of wild type or a Rubicon mutant with CT deletion was sufficient to ablate the autophagic vacuole accumulation in Rubicon depleted cells, but the expression of the Rubicon mutant with the RUN domain deletion failed to complement this phenotype (Fig. 5B and 5C). Hence, the RUN domain is crucial for Rubicon's negative function in autophagosome maturation.

The degradation of a selective autophagy substrate p62 (21,22) was also examined in Rubicon depleted and complemented cells. p62 autophagic degradation was accelerated in Rubicon depleted cells, which was rescued by complementation with wild type Rubicon and a CT deletion mutant, but not the RUN domain deletion mutant (Fig. 5D). This result is consistent with the EM results, indicating that the RUN domain of Rubicon is important for Rubicon's negative regulator role in autophagic degradation.

DISCUSSION

Rubicon is a recently identified PI3KC3 subunit that is required for suppression of autophagosome maturation. In this study, we demonstrated that Rubicon preferentially

interacts with UVRAG in the PI3KC3 endosomal subcomplex. In addition to a physical interaction with UVRAG, Rubicon also binds to the catalytic subunit hVps34 via its RUN domain. This binding contributes to its suppression of hVps34 lipid kinase activity. Finally, The RUN domain is critical for Rubicon's function in autophagosome maturation and autophagic degradation. Although the RUN domain is proposed to interact with small GTPases, here we reveal a unique role of the RUN domain in hVps34 interaction and autophagy regulation.

A list of proteins has been reported to interact with hVps34, including Rab5 (23-27). Recent biochemical purifications from several laboratories have disclosed 6-7 subunits of PI3KC3 including hVps34, p150/Vps15, Beclin 1/Atg6, UVRAG, Barkor/Atg14(L), and Rubicon (7,9-11). All of them except Rubicon have a functional counterpart in yeast. Also, similar to the yeast PI3K complex, mammalian PI3KC3 forms two mutually exclusive subcomplexes (7,9-11). One subcomplex contains the core complex, and Barkor/Atg14(L). Due to its localization on early autophagosomes and functionality in autophagosome formation (7), we refer to this complex as the autophagosomal PI3KC3 complex. The other subcomplex contains the core complex, UVRAG and Rubicon. This complex is mainly localized to endosomes; we therefore refer to it as the endosomal PI3KC3 complex. Emerging evidence suggests that this subcomplex is involved in both autophagosome and endosome maturation (9,10,12).

However, the architecture of the mammalian PI3KC3 complex is slightly different from its counterpart in yeast. For example, Barkor/Atg14(L) and UVRAG interact with hVps34 via Beclin 1 in mammalian cells (7,13), whereas two regulatory proteins Atg14 (Barkor like) and Vps38 (UVRAG-like) mediate the interaction between hVps34 and Atg6/Beclin 1 (3). Furthermore, because Rubicon, and its autophagy inhibiting functions through the PI3KC3 complex have no homologous function in yeast, the autophagy inhibition activity of Rubicon could be unique to multi-cell organisms. However, the mechanism of PI3KC3 and autophagy inhibition by Rubicon is largely unknown. Interestingly, we found no direct interaction between Beclin 1 and Rubicon, although Rubicon was named as a Beclin 1 interacting protein (9,10). Instead, Rubicon interacts with UVRAG and hVps34 directly (Fig. 2). The physical interaction between Rubicon and hVps34 might help to explain its inhibitory effect on PI3K activity. The data presented in this study support a critical role of the RUN domain in the inhibitory function of Rubicon. However, the interaction between the central region of Rubicon and UVRAG (9,10) might also contribute to the negative regulation of Rubicon, which needs further investigation. We can also not exclude the possibility that Rubicon could interact with hVps34 through region(s) other than the RUN domain. Nevertheless, our data demonstrate that the RUN domain is not only sufficient for hVPS34 binding but also critical for regulating PI3KC3 lipid kinase activity and autophagy.

The RUN domain was originally found in a group of proteins that interact with small GTPases (15-17). It was therefore proposed as a binding surface for small GTPases. Our results indicate that the RUN domain could also bind hVps34. This may provide a possible link for many RUN-domain containing proteins to PI3K regulation. The detailed mechanism of which is still largely unknown, and need to be further explored through more structural and functional analyses.

In this study, we have identified a previous unknown function of the RUN domain of Rubicon in PI3KC3 and autophagy regulation. Dissecting the molecular mechanism of this molecule will provide exciting insight into the mechanism of the autophagic pathways. Such information should be critical for the development of novel therapeutical tools for multiple human pathological conditions suffering from dysfunctions of autophagy.

References

1. Sagona, A. P., Nezis, I. P., Pedersen, N. M., Liestol, K., Poulton, J., Rusten, T. E., Skotheim, R. I., Raiborg, C., and Stenmark, H. (2010) *Nat. Cell. Biol.* 12, 362-71
2. Schu, P. V., Takegawa, K., Fry, M. J., Stack, J. H., Waterfield, M. D., and Emr, S. D. (1993) *Science* **260**, 88-91
3. Kihara, A., Noda, T., Ishihara, N., and Ohsumi, Y. (2001) *J. Cell. Biol.* **152**, 519-530
4. Kinchen, J. M., Doukoumetzidis, K., Almendinger, J., Stergiou, L., Tosello-Trampont, A., Sifri, C. D., Hengartner, M. O., and Ravichandran, K. S. (2008) *Nat. Cell. Biol.* **10**, 556-566
5. Cao, Y., and Klionsky, D. J. (2007) *Cell. Res.* **17**, 839-849
6. Obara, K., Sekito, T., and Ohsumi, Y. (2006) *Mol. Biol. Cell.* **17**,1527-1539
7. Sun, Q., Fan, W., Chen, K., Ding, X., Chen, S., and Zhong, Q. (2008) *Proc. Natl. Acad. Sci* **105**, 19211-19216
8. Itakura, E., Kishi, C., Inoue, K., and Mizushima, N. (2008) *Mol. Biol. Cell.* **19**, 5360-5372
9. Matsunaga, K., Saitoh, T., Tabata, K., Omori, H., Satoh, T., Kurotori, N., Maejima, I., Shirahama-Noda, K., Ichimura, T., Isobe, T., Akira, S., Noda, T., and Yoshimori, T. (2009) *Nat. Cell. Biol.* **11**, 385-396
10. Zhong, Y., Wang, Q. J., Li, X., Yan, Y., Backer, J. M., Chait, B. T., Heintz, N., and Yue, Z. (2009) *Nat. Cell. Biol* **11**, 468-476
11. Sun, Q., Fan, W., and Zhong, Q. (2009) *Autophagy* **5,** 713-716
12. Sun, Q., Westphal, W., Wong, K. N., Tan, I., and Zhong, Q. (2010) *Proceedings of the National Academy of Sciences of the United States of America*. In press
13. Liang, C., Feng, P., Ku, B., Dotan, I., Canaani, D., Oh, B. H., and Jung, J. U. (2006) *Nat. Cell. Biol.* **8**, 688-699
14. Liang, C., Lee, J. S., Inn, K. S., Gack, M. U., Li, Q., Roberts, E. A., Vergne, I., Deretic, V., Feng, P., Akazawa, C., and Jung, J. U. (2008) *Nat. Cell. Biol.* **10**, 776-787
15. Mari, M., Macia, E., Le Marchand-Brustel, Y., and Cormont, M. (2001) *J. Biol. Chem.* **276**, 42501-42508
16. Kukimoto-Niino, M., Takagi, T., Akasaka, R., Murayama, K., Uchikubo-Kamo, T., Terada, T., Inoue, M., Watanabe, S., Tanaka, A., Hayashizaki, Y., Kigawa, T., Shirouzu, M., and Yokoyama, S. (2006) *J. Biol. Chem.* **281**, 31843-31853
17. Recacha, R., Boulet, A., Jollivet, F., Monier, S., Houdusse, A., Goud, B., and Khan, A. R. (2009) *Structure* **17,** 21-30
18. Fan, W., Tang, Z., Chen, D., Moughon, D., Ding, X., Chen, S., Zhu, M., and Zhong, Q. *Autophagy* **6**, 614 - 621
19. Backer, J. M. (2008) *Biochem. J.* **410**, 1-17
20. Lindmo, K., and Stenmark, H. (2006) *J. Cell. Sci.* **119**, 605-614
21. Bjorkoy, G., Lamark, T., Brech, A., Outzen, H., Perander, M., Overvatn, A., Stenmark, H., and Johansen, T. (2005) *J. Cell. Biol.* **171**, 603-614
22. Komatsu, M., Waguri, S., Koike, M., Sou, Y. S., Ueno, T., Hara, T., Mizushima,N., Iwata, J., Ezaki, J., Murata, S., Hamazaki, J., Nishito, Y., Iemura, S., Natsume,T., Yanagawa, T., Uwayama, J., Warabi, E., Yoshida, H., Ishii, T., Kobayashi, A.,Yamamoto, M., Yue, Z., Uchiyama, Y., Kominami, E., and Tanaka, K. (2007) *Cell* **131**, 1149-1163
23. Stein, M. P., Feng, Y., Cooper, K. L., Welford, A. M., and Wandinger-Ness, A. (2003) *Traffic* **4**, 754-771
24. Slessareva, J. E., Routt, S. M., Temple, B., Bankaitis, V. A., and Dohlman, H. G. (2006) *Cell* **126**, 191-203
25. Simonsen, A., Lippe, R., Christoforidis, S., Gaullier, J. M., Brech, A., Callaghan, J., Toh, B. H., Murphy, C., Zerial, M., and Stenmark, H. (1998) *Nature* **394**, 494-498
26. Wurmser, A. E., and Emr, S. D. (2002) *J. Cell. Biol.* **158**, 761-772
27. Christoforidis, S., Miaczynska, M., Ashman, K., Wilm, M., Zhao, L., Yip, S. C., Waterfield, M. D., Backer, J. M., and Zerial, M. (1999) *Nat. Cell. Biol.* **1**, 249-252

FOOTNOTES

We thank Cell signaling and Abgent for Rubicon antibodies, and Livy Wilz for the critical reading of the manuscript. The work is supported by a New Investigator Award for Aging from the Ellison Medical Foundation, Hellman Family Fund and NIH RO1 (CA133228) to Q. Z.

FIGURE LEGENDS

Fig. 1. Rubicon is a part of PI3KC3 complex with UVRAG. (**A**). Cell extracts from U_2OS cells expressing ZZ-Rubicon-FLAG at physiological levels or vector alone (Con) were collected, and purified through IgG beads and FLAG M2 beads sequentially. The resulting complex was resolved by 4-12% gradient SDS-PAGE and Silver staining, and analyzed by Mass Spectrometry. The identified proteins were marked. (**B**). U_2OS cell extracts were immunoprecipitated with hVps34 or Rubicon antibodies and the resulting immunoprecipitates were analyzed for Western Blotting.

Fig. 2. Rubicon physically interacts with UVRAG and hVps34. (**A**). Full-length FLAG-tagged (F) or FLAG-His double tagged (FH) recombinant hVps34, Beclin 1, Barkor/Atg14(L). Rubicon and UVRAG were purified from baculovirus infected insect cell or transfected HEK293T cells. (**B**). Rubicon interacts directly with UVRAG and hVps34 in the purified system. Purified Rubicon-FLAG-His6 or Barkor/Atg14(L)-FLAG-His6 was first bound to NTA-Ni^{2+} beads. Purified recombinant proteins for hVps34, UVRAG and Beclin1 were then allowed to pass through the Ni-NTA beads (even lanes). Bound proteins were detected by Western-Blot using anti-FLAG antibody. The empty Ni-NTA beads were used as controls (odd lanes).

Fig. 3. Rubicon binds to hVps34 via the RUN domain. (**A**). In Rubicon, three highlighted domains were the RUN, Coiled-coil (CCD), and FYVE-like domains. FLAG tagged Rubicon WT or deletion mutants, including mutants deleting the RUN, CCD, or FYVE-like domains from full-length Rubicon, as well as three large polypeptide fragments containing the RUN domain, CCD or FYVE-like domain, were co-expressed with Myc-UVRAG in HEK293T cells. Cell extracts were immunoprecipitated with anti-FLAG antibody. The bound proteins (B for bound) or the 5% input extract were detected by immunoblotting using antibodies as indicated. (**B**) The N-terminus of Rubicon (1-300aa) was further divided into three FLAG tagged fragments containing amino acids from 1-48, 49-180 (RUN domain) and 181-300, respectively. These deletion constructs were co-expressed with Myc-hVps34 in HEK293T cells. The cell extracts were immunoprecipitated with FLAG M2 beads followed by Western Blotting for Myc-hVps34 and FLAG tagged Rubicon fragments.

Fig. 4. The RUN domain of Rubicon contributes to efficient inhibition of hVps34 lipid kinase activity. **(A).** Vector alone, the N-terminal region (1-300aa), and the C-terminal region (181-972) of Rubicon were co-expressed with GFP2xFYVE in HEK293T cells. GFP2xFYVE puncta were observed under a fluorescence microscope. **(B).** Quantitative analysis (summarized from 100 cells) of GFP2xFYVE puncta in cells described in (A). **(C).** FLAG-tagged hVps34 was co-expressed in HEK293T cells with one of these Myc-tagged proteins (Beclin 1, Barkor/Atg14(L), UVRAG, Rubicon, and Rubicon-ΔRUN). (**D**). Cell lysates from cells described in (C) were immunoprecipitated with M2 beads and assayed for PI3K kinase activity in a TLC assay. The phosphorylation product $^{[32P]}$-PI3P was separated by TLC and further visualized by a phosphorimager.

Fig. 5. The Run domain is important for autophagy suppression by Rubicon. (**A**). Rubicon shRNA non-induced U_2OS cells (4i DOX-) and doxycycline (DOX) induced RNAi depleted cells (4i DOX+) were observed under the transmission electron microscope. Autophagic vacuoles are

marked by arrows. The clone 4 expressing shRNA against Rubicon (Rubicon4i) was used in this study. Scale bar (2μm). (**B**). Parental U_2OS cells (U_2OS-TR, U_2OS cells expressing tet-repressor), Rubicon shRNA non-induced U_2OS cells (4i DOX-), RNAi depleted cells (4i DOX+), Rubicon depleted cells complemented with vector alone, Flag tagged Rubicon wild type, Rubicon CT deletion (Δaa800-972), or Rubicon RUN domain deletion (Δaa1-180) were observed under the transmission electron microscope. Autophagic vacuoles are marked by arrows. (**C**) Quantitative results (summarized from 50 cells per cell line) of autophagic vacuoles (AVs) described in (B). (**D**) Rubicon was detected by anti-Flag M2 antibody; p62 and Tubulin were detected by respective antibodies in immunoblotting in cells described in (B).

Figure 1. Sun et al.

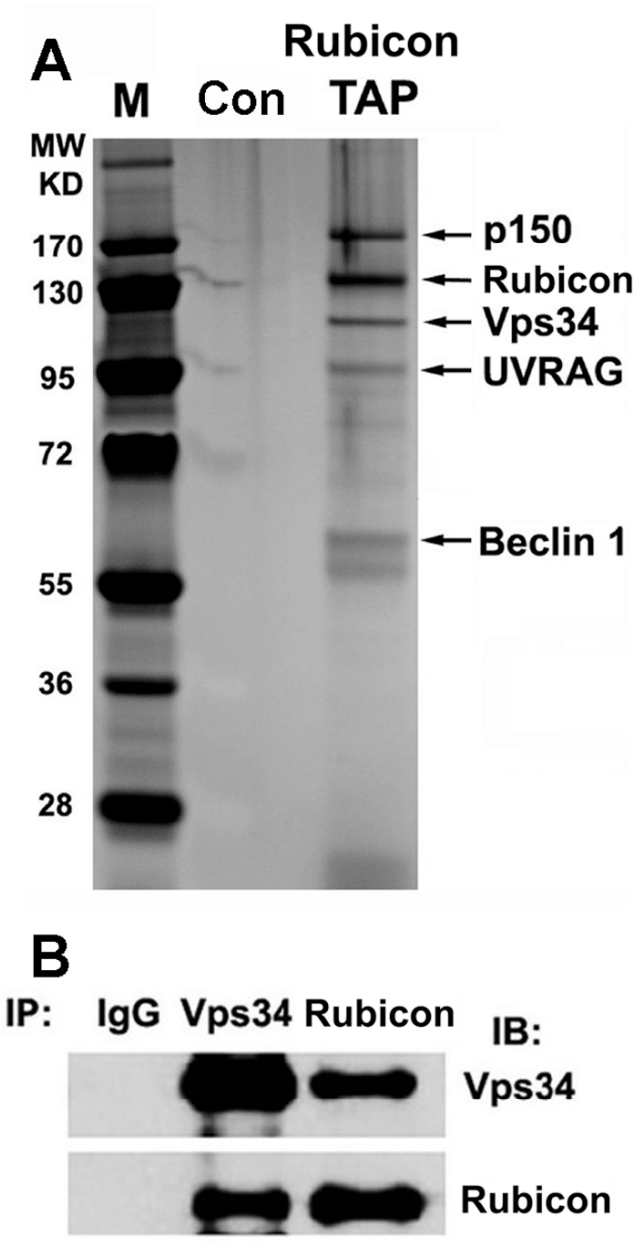

Figure 2. Sun et al.

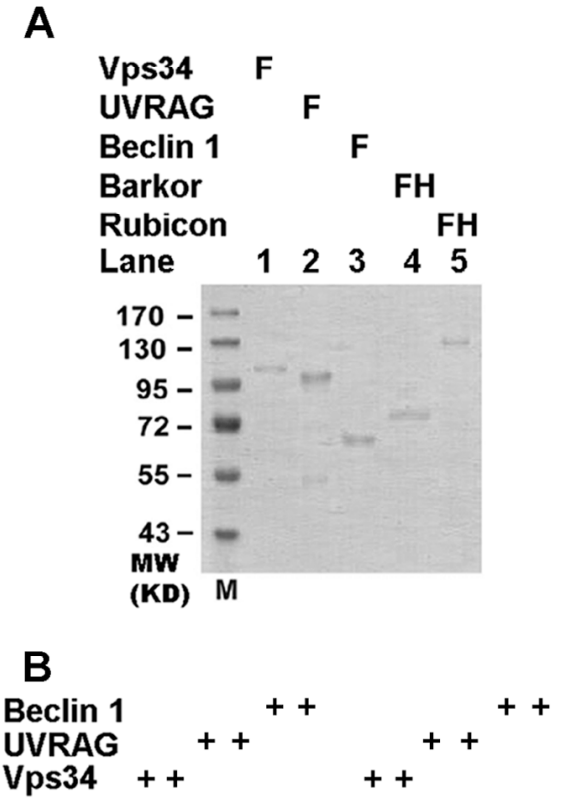

Figure 3. Sun et al.

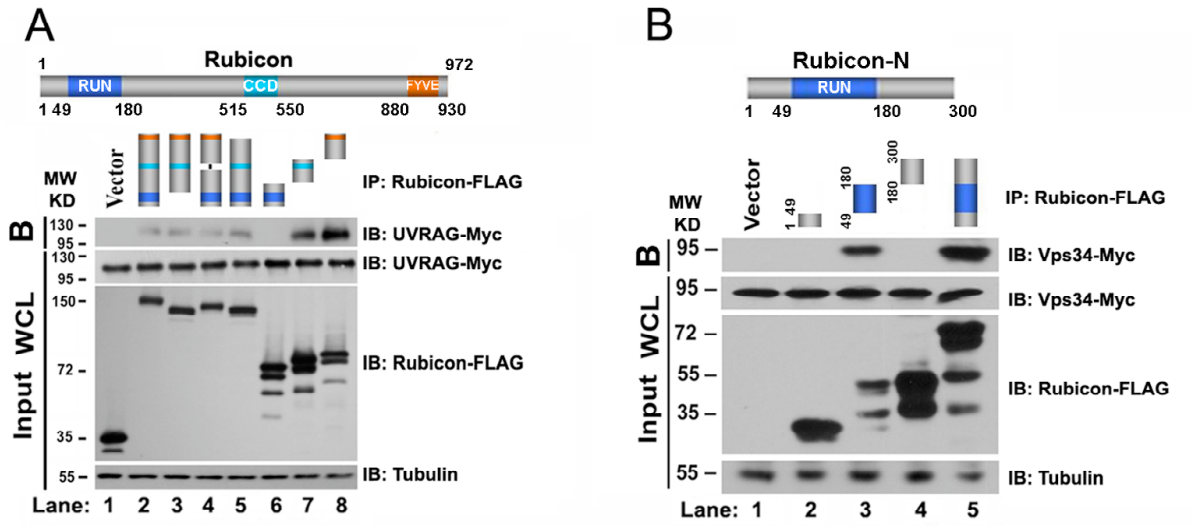

Figure 4. Sun et al.

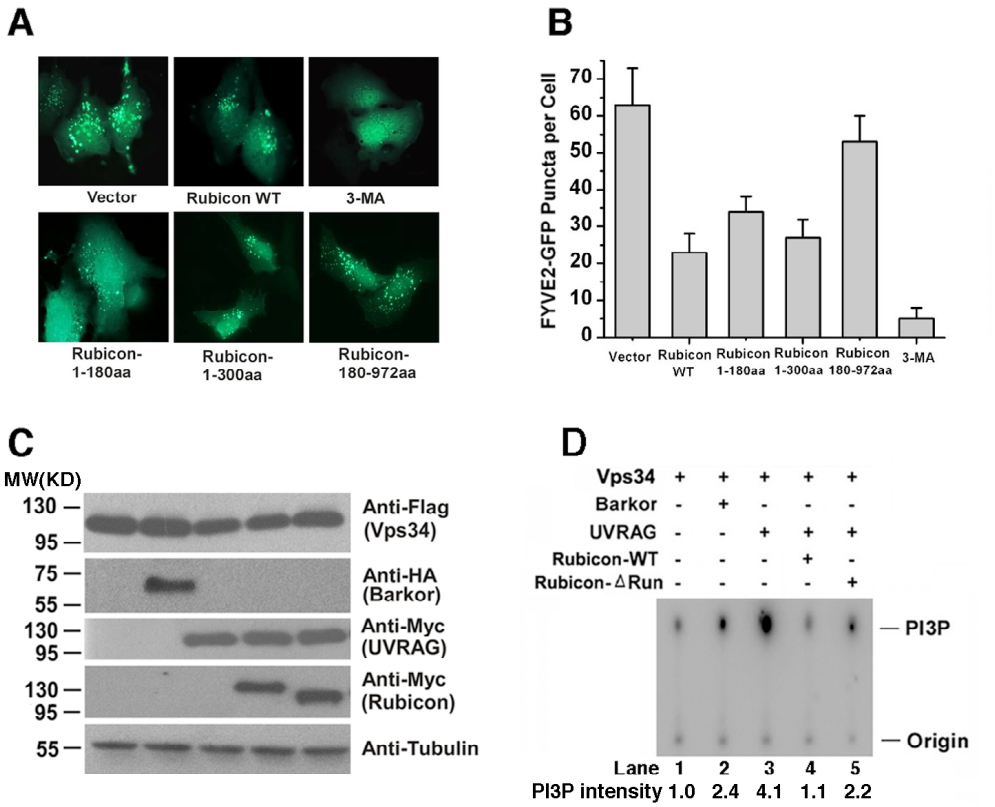

Figure 5. Sun et al.